OFFICE OF NAVAL RESEARCH

Grant #N00014-91-J-1630
R&T Code 313s002---05

Technical Report #18

Nanometer Scale Phase Separation in Mixed Composition Self-Assembled Monolayers

by

S. J. Stranick, S. V. Atre, A. N. Parikh, M. C. Wood, D. L. Allara, N. Winograd, and P. S. Weiss

Department of Chemistry
152 Davey Laboratory
The Pennsylvania State University
University Park, PA 16802

Prepared for publication in

Nanotechnology

14 July 1994

REPORT DOCUMENTATION PAGE

Form Approved
OMB No. 0704-0188

1. AGENCY USE ONLY *(Leave blank)*

2. REPORT DATE
14 July 1994

3. REPORT TYPE AND DATES COVERED
Technical 6/1/94–5/31/95

4. TITLE AND SUBTITLE
Nanometer Scale Phase Separation in Mixed Composition Self–Assembled Monolayers

5. FUNDING NUMBERS
N00014–91–J–1630

6. AUTHOR(S)
S. J. Stranick, S. V. Atre, A. N. Parikh, M. C. Wood, D. L. Allara, N. Winograd, and P. S. Weiss

7. PERFORMING ORGANIZATION NAME(S) AND ADDRESS(ES)
Department of Chemistry
152 Davey Laboratory
The Pennsylvania State University
University Park, PA 16802

8. PERFORMING ORGANIZATION REPORT NUMBER
Report #18

9. SPONSORING/MONITORING AGENCY NAME(S) AND ADDRESS(ES)
Office of Naval Research
Chemistry Program
800 N. Quincy Street
Alexandria, VA 22217–5000

10. SPONSORING/MONITORING AGENCY REPORT NUMBER

11. SUPPLEMENTARY NOTES
Prepared for publication in *Nanotechnology*

12a. DISTRIBUTION/AVAILABILITY STATEMENT
Approved for public release.
Distribution unlimited.

12b. DISTRIBUTION CODE

13. ABSTRACT *(Maximum 200 words)*

Mixed composition monolayers of similar *n*–alkanethiols on Au{111} are formed by self–assembly. While the average surface composition of these films accurately reflects the composition of the deposition solution, scanning tunneling microscopy and secondary ion mass spectroscopy measurements show that the films phase separate on the nanometer scale. Scanning tunneling microscopy has been used to follow molecular motions within these films. We discuss our observations in terms of the formation and stability of the phase segregated domains, and their potential importance in nanoscale applications.

14. SUBJECT TERMS

15. NUMBER OF PAGES
15 pages

16. PRICE CODE

17. SECURITY CLASSIFICATION OF REPORT	**18. SECURITY CLASSIFICATION OF THIS PAGE**	**19. SECURITY CLASSIFICATION OF ABSTRACT**	**20. LIMITATION OF ABSTRACT**
Unclassified	Unclassified	Unclassified	UL

NANOMETER SCALE PHASE SEPARATION IN MIXED COMPOSITION SELF-ASSEMBLED MONOLAYERS

S. J. Stranick, S. V. Atre, A. N. Parikh, M. C. Wood, D. L. Allara, N. Winograd, and P. S. Weiss*

Abstract

Mixed composition monolayers of similar *n*-alkanethiols on Au{111} are formed by self-assembly. While the average surface composition of these films accurately reflects the composition of the deposition solution, scanning tunneling microscopy and secondary ion mass spectroscopy measurements show that the films phase separate on the nanometer scale. Scanning tunneling microscopy has been used to follow molecular motions within these films. We discuss our observations in terms of the formation and stability of the phase segregated domains, and their potential importance in nanoscale applications.

☒
☐
☐

Dist. ibution /	
Availability Codes	
Dist	Avail and / or Special
A-1	

S. J. Stranick, M. C. Wood, N. Winograd and P. S. Weiss, Department of Chemistry, The Pennsylvania State University, University Park, PA 16802, USA.

S. V. Atre and A. N. Parikh, Department of Materials Science and Engineering, The Pennsylvania State University, University Park, PA 16802, USA.

D. L. Allara, Departments of Chemistry and Materials Science and Engineering, The Pennsylvania State University, University Park, PA 16802, USA.

---

*To whom correspondence should be addressed.

Fax: (814) 863–8081. E-mail: stm@psuvm.psu.edu.

Submitted to
Nanotechnology

14 July 1994

I. Introduction

As the applications of alloys and composite materials extend into the realm of nanotechnology, an understanding of the properties and behavior of these materials on the molecular scale will become of paramount importance. Critical aspects of these materials are the determination of the nanometer scale structures formed from multicomponent films and the extent to which these structures can be controlled and stabilized. Here we address the issue of phase separation in mixed composition systems. To this end, we have studied two component quasi–two–dimensional self–assembled monolayers (SAMs) of *n*–alkanethiols on Au{111}.

Densely packed, crystalline self–assembled monolayers of *n*–alkanethiols on Au{111} spontaneously form when a Au{111} surface is immersed in a solution containing *n*–alkanethiols [1]. These quasi–two–dimensional organic monolayer films are formed by covalently bonding the thiol S to the Au surface, while the alkyl chains interact through van der Waals forces to form an ordered overlayer. The terminal functional groups of the alkyl chains define the exposed surface of this self–assembled organic layer [1,2]. By varying the functionality of these end groups, the physicochemical nature of the surface can also be varied. It is shown below how the terminal functional groups used in this study, $-CH_3$, $-CO_2CH_3$, $-OH$, and $-CN$, determine the structural properties and phase behavior of this system. The *n*–alkanethiols used — $CH_3(CH_2)_{15}SH$, $CH_3O_2C(CH_2)_{15}SH$, $HOCH_2(CH_2)_{15}SH$, and $NCCH_2(CH_2)_{15}SH$ — have nearly identical chain lengths and differ only in their terminal functional groups. These slight variations result in the formation and growth of phase segregated nanometer scale molecular domains.

Direct observation of phase segregation in Langmuir films by techniques other than the scanning probe microscopies have previously been limited to macroscopic domains [3]. Meyer and coworkers have used frictional force microscopy to study phase segregation in Langmuir–Blodgett films in which two very different component molecules are co–deposited [4,5]. In a series of experiments they have shown how the domain shapes in these relatively mobile films (prior to deposition) depend on alkyl chain length of one of the components [5]. We have used scanning tunneling microscopy (STM) to demonstrate phase segregation at the molecular scale in varied composition, two–component SAMs [6,7]. The spatial distribution of the molecules comprising the phase–separated domains as well as the temporal evolution of these structures were observed [6]. The formation and growth of these domains has been observed in time lapse STM imaging [8].

In a recent theoretical and experimental treatment of molecular phase segregation in mixed composition self–assembled monolayers of $CH_3(CH_2)_{11}SH$ and $CH_3(CH_2)_{21}SH$, Folkers *et al.* concluded that, in general, a SAM in equilibrium with the deposition solution will be comprised of a single phase of either a pure thiol or a heterogeneous mixture of the two thiols [9]. Folkers *et al.* also pointed out that if exchange between the film and the solution is incomplete (*i.e.* the sample is removed from solution before equilibrium is reached), then the film may form phase–separated islands [9]. This is certainly the situation in our sample preparation. While the length of time that our samples remain in the solution are an order of magnitude *longer* than typical immersion times, results of imaging time–of–flight secondary ion mass spectroscopy (TOF–SIMS) studies have shown that the rates of exchange between the solution and the monolayer film are extremely slow at room temperature [10]. In these studies partial and complete monolayers have been immersed in solutions of different thiols and then the films have been analyzed using SIMS. Only in the case where thiols from the initial exposure were not on the surface (*e.g.* where they had been mechanically removed), were the thiol species from the second exposure found in abundance [10]. In ref. [9], Folkers *et al.* raised the deposition solution temperature to 60°C to accelerate SAM–solution exchange in order to attempt to reach equilibrium, but could not ascertain whether they had done so.

We have also acquired evidence using TOF–SIMS that for some mixed composition SAMs the distribution of neighbor molecules within the film are not random. This is a natural result of phase separation — molecules are more likely to be found near identical molecules than if they were mixed randomly (in which case the probabilities on all length scales would be given by the surface density of each molecule).

In this paper we discuss the preference of these similar alkanethiol self–assembled system to phase segregate. The presence of these phase separated domains indicates that the equilibrium structures of these film compositions are phase separated on some length scale.

II. Experimental Section

Substrates for this study were prepared by evaporation of gold (99.999%) onto the surface of freshly cleaved mica which was preheated in vacuum to ~340°C [11]. The base pressure in the chamber during evaporation was $\leq 6 \times 10^{-7}$ torr. After ~100 nm of gold was deposited, the substrate temperature was returned to <40°C while still under vacuum, then the chamber was back–filled with purified nitrogen, the substrates removed, and immersed immediately into ethanolic solutions of either $CH_3(CH_2)_{15}SH$, $CH_3O_2C(CH_2)_{15}SH$, $HOCH_2(CH_2)_{15}SH$, $NCCH_2(CH_2)_{15}SH$, or a combinations of two of these thiols at 1m<u>M</u> total thiol concentration. In this study, pure solutions of each thiol and mixed solutions of pairs of thiols were examined. At these concentrations, the thiols are soluble in ethanol, and readily form homogeneous solutions. The substrates were immersed in the solutions for 4 days at room temperature, after which the samples were withdrawn, rinsed extensively in ethanol, and dried under a stream of nitrogen. Mica–supported samples were analyzed using STM. Companion samples prepared on gold films on native oxide–covered single crystal Si(100) wafers (as described elsewhere [12]) were characterized by X–ray photoelectron spectroscopy (XPS), ellipsometry, and infrared spectroscopy (IRS) to verify the quality, thickness and composition of the self–assembled films [2,13]. Samples prepared on gold–coated Si wafers were also studied using TOF–SIMS in the static regime (low total ion dose). The imaging TOF–SIMS instrument has been described elsewhere [14]. These samples were analyzed immediately after removal from ethanol, rinsing, and drying. The monolayer films were observed to be stable in air for the duration of the experiments with no evidence for the formation of sulfonates or other degradation products as shown by XPS, IR, and SIMS.

The STM images were recorded in air using a microwave–frequency–compatible beetle–style scanning tunneling microscope [15]. All the samples were studied use DC tunneling current to control the tip–sample separation. All images were recorded at tunneling gap impedances that ensured a large tip–sample separation, $10^9\Omega$. All STM images were recorded in constant tunneling current mode and are presented unfiltered. The tunneling current was 2 nA with a tip bias voltage of $^{-}2$V. The STM piezoelectric scanner calibrations are performed by recording atomic resolution images of surfaces of known crystallography.

The mechanism that allows nominally insulating organic films to be imaged remains unclear. Dürig *et al.* have conducted simultaneous STM and atomic force microscopy (AFM) experiments on SAMs of $HO(CH_2)_{16}SH$ on gold [16]. From these simultaneous measurements, they concluded that the pressure induced by the probe tip must play an important role in the ability of electrons to tunnel through these films. Other studies have shown how the presence of "insulating" adsorbates assists in the tunneling of electrons in the STM tunnel junction without the need for compressing adsorbates [17].

We have previously shown how STM can be used to determine the distribution of mixed composition self–assembled films of *n*–alkanethiol molecules, $CH_3(CH_2)_{15}SH$ and $CH_3O_2C(CH_2)_{15}SH$, on Au{111} [6,7]. After imaging single composition films and characterizing the features (such as point defects) found in STM images, we imaged mixed composition SAMs with 1:3, 1:1, and 3:1 ratios of the two thiols [6–8]. The most striking features were the presence of nanometer scale domains that were differentiated in topographic images. The two molecular domains appeared at 1Å height difference in constant current images at $10^9\Omega$ gap impedance. In each case, the ratio of the areas of the domains was found to be equal to the ratio of the two thiols in the deposition solutions. Based on the analysis of the areas and the strong correlation with the expected surface concentrations, we assigned these topographic features as domains of the two thiolate species in the films.

III. Results

Shown in Fig. 1 is a scanning tunneling microscope image of a 450Åx450Å region of a self–assembled monolayer of a 1:1 ratio of $CH_3O_2C(CH_2)_{15}SH$ and $CH_3(CH_2)_{15}SH$ on Au. The phase separated domains appear as regions 1Å different in height from the neighboring domains of the other thiolate moiety. From our previous studies of various composition ratios [6,7], we are able to assign the higher of the two domains to the methyl–ester–terminated molecule. These domains are highly intertwined which results in them being long and relatively narrow. This is discussed further in Section IV below.

As seen in the STM images, the distribution of molecules on the surface is clearly not random and thus should be evident in surface spectroscopies. To this end, we have explored the nanometer length scale distributions by TOF–SIMS. The spot size of the ion beam used for imaging currently has a lower limit of ~500Å [14], too large to identify phase separated domains of the size shown in Fig. 1. Indeed, no phase separation is observed by direct TOF–SIMS imaging. Instead, we use the propensity of nearby adsorbed molecules to be ejected simultaneously from the collision cascade due to single ion impacts. The higher effective "resolution" in this case results from the localization of the collision cascade. Nearby adsorbates then are either desorbed bound together or recombine in the gas phase in the vicinity of the surface. Recent molecular dynamics simulations show that the lateral sensitivity in such a measurement is ~20Å [14,18].

Fig. 2 shows the SIMS spectra for 9:1, 1:1, and 1:9 mixtures of $CH_3(CH_2)_{15}SH$ and $HOCH_2(CH_2)_{15}SH$ in the region where ions composed of two thiolate species bound to a single Au atom are found. Fig. 3 shows the SIMS spectra for 9:1, 1:1, and 1:9 mixtures of $HOCH_2(CH_2)_{15}SH$, and $NCCH_2(CH_2)_{15}SH$ in the equivalent spectral region. As noted above, we interpret the presence of these ions as being due predominantly to two thiolate species being simultaneously ejected during the same collision cascade from a single incident (Ga^+) ion. By analyzing the areas of the mixed thiolate ions — the central peaks in the spectra — we can determine the extent to which one thiolate is surrounded by a purely statistical distribution of each thiol or whether the surface is patterned on this ~20Å length scale. Analysis of the SIMS data indicates that the mixtures shown in Fig. 2 are patterned whereas those shown in Fig. 3 are consistent with a statistical distribution of thiolates. The integrated area of the mixed thiolate negative ion ($CH_3(CH_2)_{15}S–Au^-–S(CH_2)_{15}CH_2OH$) for the 1:1 ratio film in Fig. 2 (spectrum b) is reduced by a factor of 1.6 from what would be found for a statistical distribution of molecules within the film, and is reduced by a factor as high as 4.9 for a 9:1 ratio film (spectrum a). By careful analysis of these integrated intensities we expect to be able to quantify the fraction of the surface covered by "interface lines" vs. the fraction covered by pure domains of one molecule.

Mixed composition SAMs show greatly reduced defect densities compared to the single composition films that we have studied prepared under identical deposition conditions [6]. We have tentatively assigned this to the interface tension that is a consequence of the differing intermolecular interactions. Thus a quantitative measurement of the fraction of the surface covered by interface would be an important parameter in the preparation of nearly ideal films.

IV. Discussion

We have previously shown how molecules exchanging between domains within the film can account for some portion of domain formation and growth [6]. The observed time scale of this exchange is quite slow (*ca.* 1 exchange per site per hour), but the actual growth rate is most likely faster. This is explained by the initial stages of 2–D domain growth being at or along the interfaces which is much more rapid than the later part of growth. Consider an initially random mixture within the film with the cross–interaction between adsorbates A and B lower than that of either like intermolecular attraction A–A or B–B. Such a system starts out in a high energy configuration because it has a high total interface length and thus a large contribution from the many A–B interactions. It then evolves to lower energy configurations (towards thermodynamic equilibrium), by reducing the interface length and thus interface energy through the growth of increasingly larger domains. Finally, the system moves relatively slowly through its final "annealing" stage where smaller domains merge to form larger ones. This consumption of smaller domains results in a reduction of the overall interfacial energy and has been observed in time lapse STM imaging [6]. We have observed the reduction of domain curvature by molecular exchange between domains. These observations lend support to the interfacial energy reduction argument presented above.

In the 1:1 samples we see that in STM images the domains are highly connected, but relatively narrow. In the 1:3 methyl–terminated to methyl–ester–terminated samples the methyl–ester–terminated domains are also extended and nearly continuous. In the complementary 3:1 mixture, the majority methyl–terminated phase shows no apparent propensity to form extended domains. These observations allow us to rank the relative strengths of the sampled interactions. The cross–interaction between methyl–terminated molecules and methyl–ester–terminated molecules is lower than either of the like molecule attractions. Further, the methyl ester to methyl ester intermolecular attraction is stronger than that for the methyl–terminated molecules.

V. Conclusions and Future Prospects

The techniques of scanning tunneling microscopy and secondary ion mass spectroscopy have allowed us to probe the nanometer scale structure and stability of mixed composition self–assembled monolayers of *n*–alkanethiols on Au{111}. Using these binary films, we have shown that mixed composition self–assembled monolayers of even very similar alkanethiols on Au{111} phase separate into nanometer scale domains of each component. These observations aid in the development of a fundamental understanding of the formation of nanometer scale domains and in the application of mixed composition self–assembled monolayers to the generation and stabilization of spatial patterns of adsorbed molecules. We note that these naturally formed patterns and structures can be used as a basis for further creation of nanometer scale structures [19].

We are currently attempting to create varying nanometer scale surface structures by changing our deposition strategies and by post–deposition modification of the terminal functional groups exposed on the SAM. We are continuing our efforts to measure quantitatively the surface interface density using SIMS.

ACKNOWLEDGMENTS

The authors would like to thank Michael Cygan, Doug Doren, Barbara Garrison, Sanat Kumar, Ernst Meyer, Bruno Michel, and John Vickerman for helpful discussions and Kyle Krom for help in the preparation of the figures. The authors gratefully acknowledge the National Science Foundation Chemistry, Materials Research, and Presidential Young Investigator Programs, the Office of Naval Research, the Biotechnology Research and Development Corporation, and the Shell Foundation for supporting this research.

REFERENCES AND NOTES

1 Dubois L H and Nuzzo R G 1992 *Annu. Rev. Phys. Chem.* **43** 437, and references therein

2. Nuzzo R G, Dubois L H and Allara D L 1990 *J. Am. Chem. Soc.* **112** 558

3. Von Tscharner V and McConnell H M 1981 *Biophys J* **36** 409

Heckl W M and Möhwald H 1986 *Ber. Bunsenges. Phys. Chem.* **90** 3249

4. Overney R M, Meyer E, Frommer J, Brodbeck D, Lüthi R, Howald L, Güntherodt H–J, Fujihara M, Takano H and Gotoh Y 1992 *Nature* **359** 133

Frommer J, Lüthi R, Meyer E, Anselmetti D, Dreier M, Overney R, Güntherodt H–J and Fujihira M 1993 *Nature* **364** 198

5. Meyer E, Overney R, Lüthi R, Brodbeck D, Howald L, Frommer J, Güntherodt H–J, Wolter O, Fujihara M, Takano H and Gotoh Y 1992 *Thin Solid Films* **220** 132

6. Stranick S J, Parikh A N, Tao Y–T, Allara D L and Weiss P S 1994 *J. Phys. Chem.* In press

7. Stranick S J, Kamna M M, Krom K R, Parikh A N, Allara D L and Weiss P S 1994 *J. Vac. Sci. Technol. B* **12** 2004

8. Stranick S J, Parikh A N, Allara D L and Weiss P S Submitted for publication

9. Folkers J P, Laibinis P E, Whitesides G M and Deutch J 1994 *J. Phys. Chem.* **98** 563

10. Collard D M and Fox M A 1991 *Langmuir* **7** 1192

Frisbie C D, Wollman E W, Martin J R and Wrighton M S 1993 *J. Vac. Sci. Technol. A* **11** 2368

Wood M C, Atre S V, Winograd N, Liedberg B, and Allara D L To be published

11. Chidsey C E D, Loiacono D N, Sleater T and Nakahara S 1988 *Surf. Sci.* **20** 45

Hallmark V M, Chiang S, Rabolt J F, Swalen J D and Wilson R J 1987 *Phys. Rev. Lett.* **59** 2879

Widrig C A, Alves C A and Porter M D 1991 *J. Am. Chem. Soc.* **113** 2805

12. Nuzzo R G, Fusco F A and Allara D L 1987 *J. Am. Chem. Soc.* **109** 2358

Troughton E B, Bain C D, Whitesides G M, Nuzzo R G, Allara D L and Porter M D 1988 *Langmuir* **4** 365

13. Laibinis P E, Whitesides G M, Allara D L, Tao Y–T, Parikh A N and Nuzzo R G 1991 *J. Am. Chem. Soc.* **113** 7152

14. Winograd N 1993 *Anal. Chem.* **65** 622A

15. Besocke K 1987 *Surf. Sci.* **181** 145

    Frohn J, Wolf J F, Besocke K and Teske M 1989 *Rev. Sci. Instrum.* **60** 1200

    Stranick S J and Weiss P S 1994 *Rev. Sci. Instrum.* **65** 918

16. Dürig U, Züger O, Michel B, Häussling L and Ringsdorf H 1993 *Phys. Rev. B* **48** 1711

17. Eigler D M, Weiss P S, Schweizer E K and Lang N D 1991 *Phys. Rev. Lett.* **66** 1189

    Weiss P S and Eigler D M 1993 *Phys. Rev. Lett.* **71** 3139

    Weiss P S 1994 *Trends Anal. Chem.* **13** 61

18. While the area of damage from a single ion impact has a radius of $\sim 50Å$, in molecular dynamics simulations such as those described in ref. [14], the directions of the ejected particles from a single ion impact are such that only particles ejected within $\sim 20Å$ are likely to recombine.

19. Stranick S J, Kamna M M and Weiss PS 1994 *Nanotech.* In this issue

FIGURE CAPTIONS

1. A scanning tunneling microscope image showing a 450Åx450Å area of a self-assembled monolayer of a 1:1 ratio of $CH_3O_2C(CH_2)_{15}SH$ and $CH_3(CH_2)_{15}SH$ on Au{111}. The image was recorded in constant current mode at a tunneling current of 2 nA and a tip bias voltage of $^{-}2$V. The vertical scale shows a 3Å range in topography. On the left side of the image is a monatomic height step in the Au substrate. The image is shown unfiltered.

2. Secondary ion mass spectra of mixed composition self-assembled monolayers of $CH_3(CH_2)_{15}SH$ and HO–$CH_2(CH_2)_{15}SH$ on Au for nominal mixtures of: a) 9:1, b) 1:1, and c) 1:9. The region shown once again includes the ions composed of two thiolates and one Au atom. The suppressed peak intensity of the central set of peaks in b) indicates that the thiolates are *not* randomly distributed within the film as described in the text. The spectra are offset for clarity.

3. Secondary ion mass spectra of mixed composition self-assembled monolayers of HO–$CH_2(CH_2)_{15}SH$ and NC–$CH_2(CH_2)_{15}SH$ on Au for nominal mixtures of: a) 9:1, b) 1:1, and c) 1:9. The region shown includes the ions composed of two thiolates and one Au atom. The peak intensities are in each case consistent with randomly distributed molecules within the film. The spectra are offset for clarity.

Stranick et al. Fig. 1 Up^

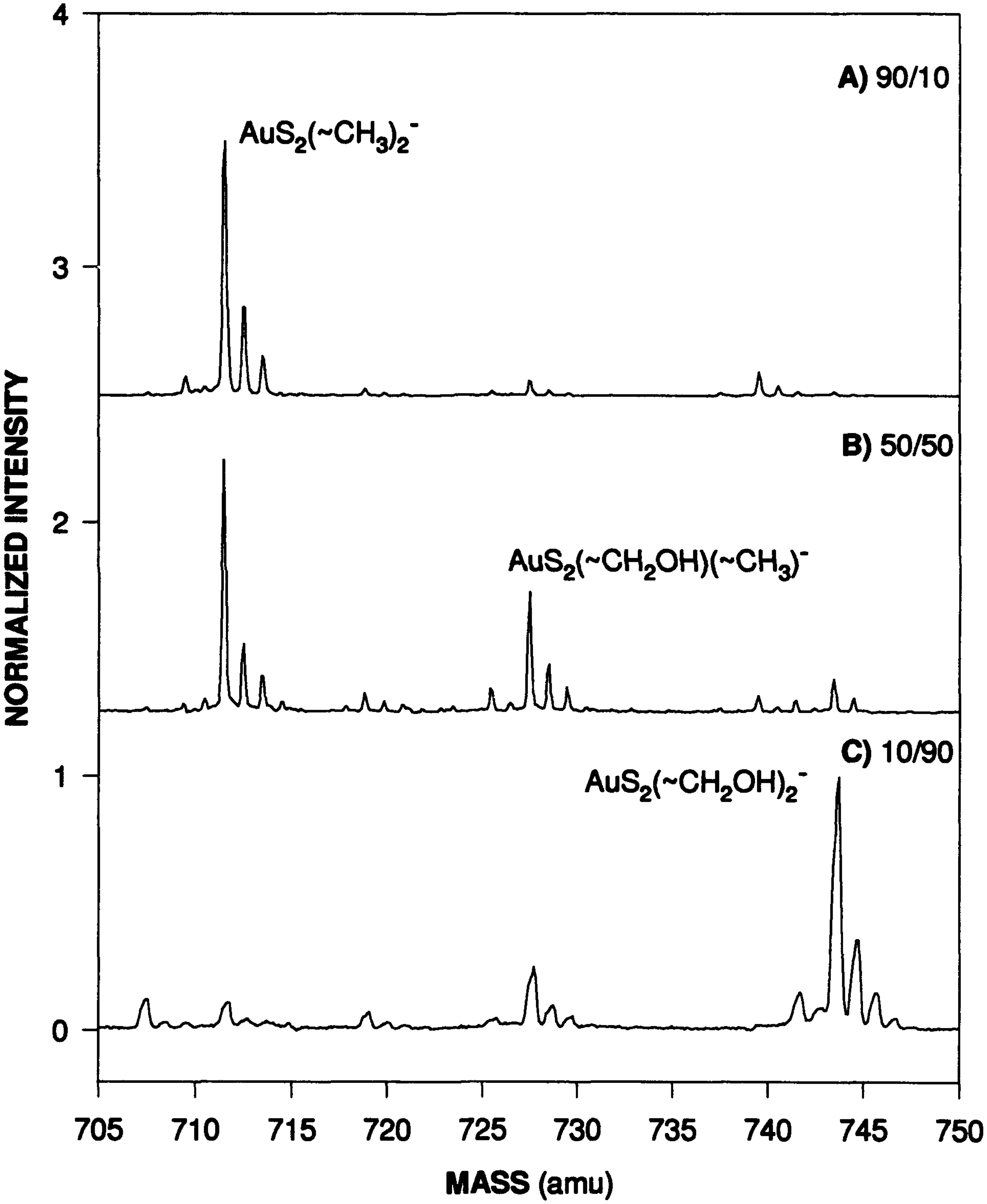

4
3
2
1
0
NORMALIZED INTENSITY
A) 90/10
$AuS_2(\sim CH_3)_2^-$
B) 50/50
$AuS_2(\sim CH_2OH)(\sim CH_3)^-$
C) 10/90
$AuS_2(\sim CH_2OH)_2^-$
705
710
715
720
725
730
735
740
745
750
MASS (amu)

Fig. 2

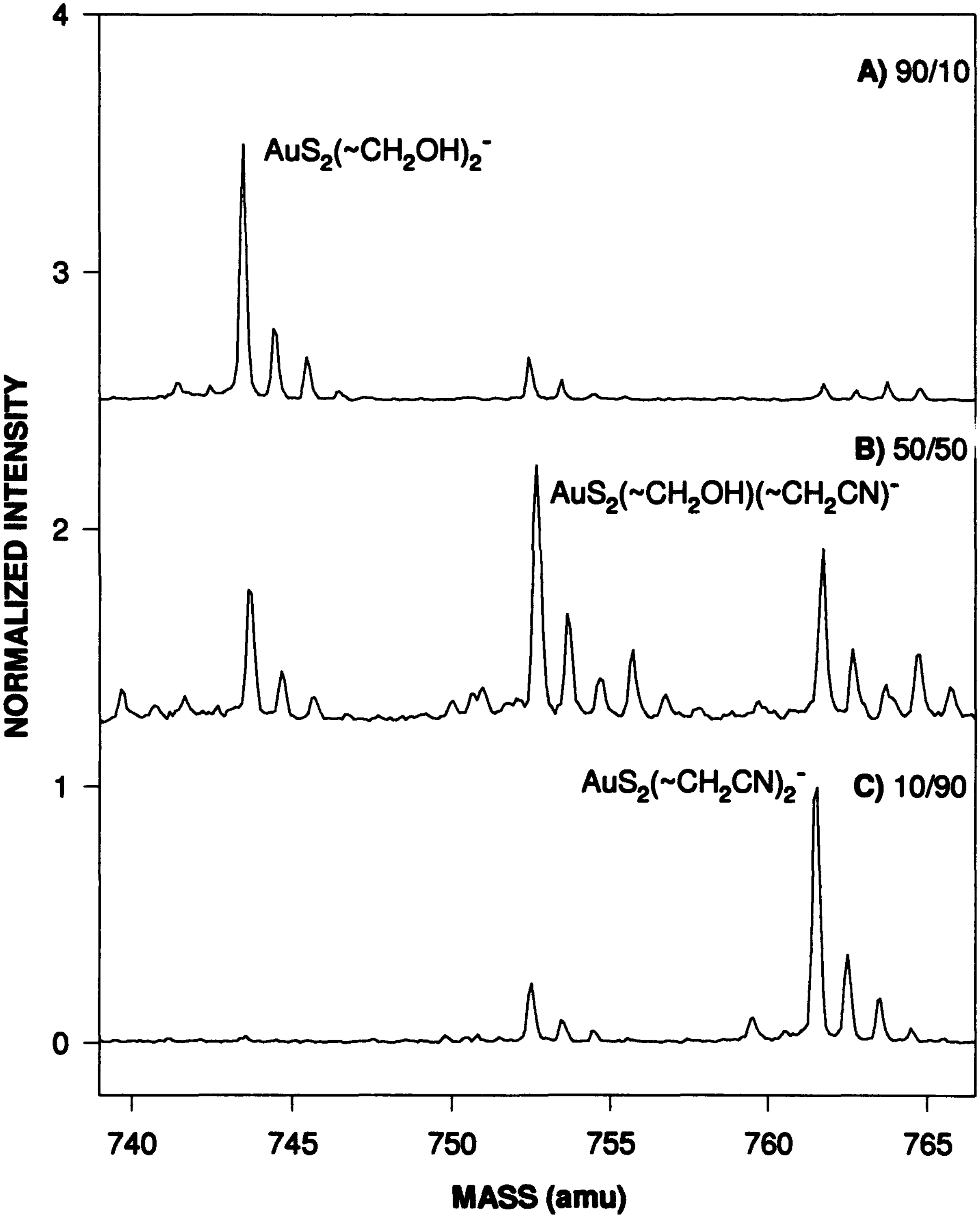
A) 90/10
$AuS_2(\sim CH_2OH)_2^-$
B) 50/50
$AuS_2(\sim CH_2OH)(\sim CH_2CN)^-$
C) 10/90
$AuS_2(\sim CH_2CN)_2^-$
NORMALIZED INTENSITY
0
1
2
3
4
740
745
750
755
760
765
MASS (amu)

Fig. 3